Acoustical analysis of an indoor test facility for aircraft Gatling guns

Matthew D. Shaw[a] and Kent L. Gee[b]

(Received: 24 February 2010; Revised: 28 August 2010; Accepted: 31 August 2010)

An indoor test facility for 20-mm and 30-mm aircraft Gatling guns was recently constructed at Hill Air Force Base in Layton, UT. In designing the range, the primary concerns were that the 30-mm gun muzzle blast overpressures were large enough to a) cause significant spallation of the concrete walls during the anticipated 20-year building usage, and b) potentially pose an auditory risk for personnel working elsewhere in the test range building. This project consisted of three phases. First, levels, directivity, and geometric spreading of the 30-mm gun blast were characterized in outdoor measurements. Second, range impulse response estimates generated by a commercial room acoustics package were used to discover potential problem areas within the range and explore the effectiveness of treatments. Finally, data were collected on gun blasts in the completed range to confirm that the test facility meets all acoustical and occupational safety requirements. ***© 2010 Institute of Noise Control Engineering.***

Primary subject classification: 21.3.6; Secondary subject classification: 73

1 INTRODUCTION

Muzzle blasts from large-caliber weapons have been the subject of acoustical and fluid-dynamical studies for several decades. Studies have included optical imaging[1] and computational modeling[2] of a muzzle blast flow field and the acoustic field[3]. Noise studies have focused on attenuation of the blast[4], reduction of community impact[5], and the effect of the blasts on surrounding objects, including aircraft structures and equipment[6].

Many military aircraft (the F-16, e.g.) employ Gatling guns as part of their weapons systems. After a gun is removed from its aircraft for servicing, it is calibrated and tested before reinstallation. The potency of these guns and the high acoustic levels require special considerations, e.g., they cannot be fired in ordinary test ranges meant for small weapons nor can they easily be fired in an outdoor test site on-base. Until recently, A-10 Warthog 30-mm gun servicing operations at Hill Air Force Base (AFB) in Layton, UT, have required personnel to transport the guns to the outdoor Utah Test and Training Range (UTTR) for testing and calibration (approximately 4.5 hrs round trip). In order to improve efficiency, it was decided to build an indoor test range on base was proposed for the GAU-8 Avenger, the Warthog's 30-mm Gatling gun. Because Hill AFB also services other aircraft, the range design included capability for testing both hydraulic and electric 20-mm guns used by the F-16, F-22, and AH-1 Cobra helicopter. The range was designed and built by HHI Corporation to Farmington, UT.

The concept of such a test range at Hill AFB was not new. Previously, a similar enclosure had been built to test 20-mm guns. However, the concrete walls of the test range began to spall and crack from repeated exposure to the high-intensity muzzle blasts. The idea of building an indoor test range for the (louder) 30-mm gun was explored in 1985[7], but it was deemed impractical for two reasons. First, measurements conducted suggested astounding pressures near the gun in excess of 620 kPa (90 psi, 210 dB). In addition, the desire to rapidly expel exhaust gases from the range could result in leakage paths to the outside and possibly significant noise transmission.

Several factors influenced the design of the facility described in this article. First, the building needed to function as a test range for at least twenty years. Consequently, HHI engineers desired to limit the peak pressures at concrete surfaces to less than 3 psi (20 kPa, 180 dB) to prevent spallation. This limit was calculated using standard structural engineering calculations for the maximum "rolling" load on rebar-reinforced, 4000–5000 psi concrete with a 12-inch thickness. Second, given the harsh environment of the firing range, acoustical treatments needed to be cost-effective, easily replaceable, and flame retardant. Finally, because the new structure would also house a machine shop adjacent to the

[a] Department of Physics and Astronomy, Brigham Young University, N283 ESC, Provo, UT 84602, email: mdshaw16@gmail.com.

[b] Department of Physics and Astronomy, Brigham Young University, N243 ESC, Provo, UT 84602, email: kentgee@byu.edu.

test range, the range transmission loss had to be sufficient to prevent personnel from being exposed to high acoustic levels.

In order to assist in the design and treatment of the new building, a characterization of the gun's acoustics and estimates of its performance in the range were required. Because of concerns with instrumentation and experimental methods from the 1985 study[7], new measurements of the gun were required. Consequently, the objectives of this research were to (a) characterize the noise from the 30-mm gun, (b) provide recommendations for acoustical treatments inside the test facility, and (c) conduct measurements to ensure that the building met the design requirements during test range operation.

2 GUN CHARACTERIZATION

2.1 Outdoor Measurements

The General Electric GAU-8 Avenger (nicknamed the "tank killer") is a 30-mm, 7-barrel Gatling gun and is the primary weapon of the A-10 Thunderbolt II "Warthog" aircraft. The gun is capable of firing 4200 rounds per minute with a muzzle exit velocity of 1070 m/s (approximately Mach 3). Pictures of the Avenger[8], along with empty shells from the 20- and 30-mm guns are displayed in Fig. 1. This gun was selected as the topic of study because it is the largest of the guns to be tested in the facility and, therefore, the most likely to cause damage to the concrete surfaces. In order to predict the pressures incident on the walls and elsewhere, it was necessary to characterize the noise from the gun in an open environment.

The tests were conducted at the 30-mm gun test site at the Oasis station of the UTTR in November 2007. Data were acquired with National Instruments PXI-4461 and PXI-4462 cards housed in an 18-slot PXI-1045 chassis. The cards permit simultaneous sampling of multiple channels at 204,800 samples per second with 24-bit resolution. The PXI chassis was linked to a laptop via an ExpressCard interface, and the data were streamed to both the internal laptop hard drive and to an external RAID hard drive. A pure sine-wave inverter was used to provide AC power for the data acquisition system in order to eliminate electrical noise often produced by a standard modified sine-wave inverter.

Two types of sensors were used for the tests. Near the gun, piezoresistive pressure transducers (Dytran 2300V3 and PCB 112A23) were mounted on tripods at the same height as the gun (1.1 m, 3.5 ft). At greater distances, 6.35-mm (40BD and 40BH) and 3.18-mm (40DP) GRAS type 1 pressure microphones were used. For the prepolarized microphones, 10 mA constant-current excitation was provided by the PXI. At 9.1 m (30 ft) and beyond, the sensors were located at a height of

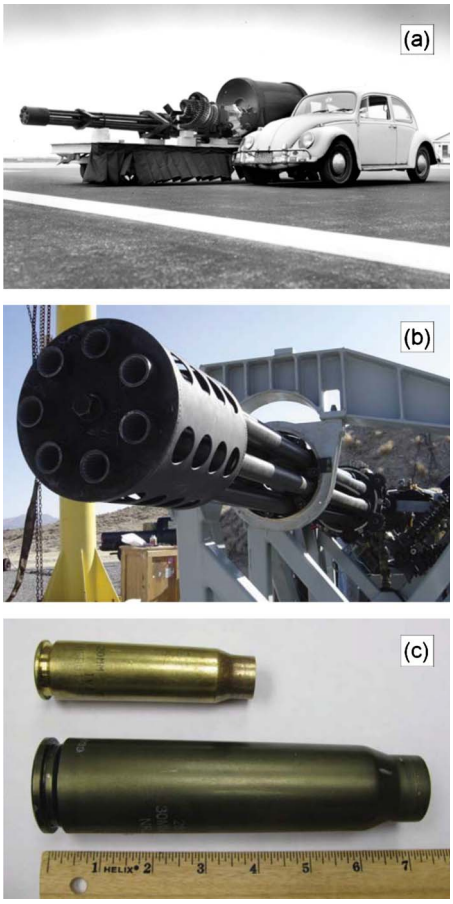

Fig. 1—Pictures of the GAU-8 Avenger; (a) The gun as it would be mounted on the aircraft[8]; (b) The front of the gun, showing the lack of a muzzle device; (c) Empty shells for both the 20-mm and 30-mm guns.

4.1 m (14 ft) in order to facilitate separation in time of the direct and ground-reflected blasts. The heights of the closer microphones were adjusted to yield a straight ray between the gun muzzle and the 30 ft microphones. A schematic of the composite sensor layout is shown in Fig. 2. The black arrow in the figure denotes the firing direction and 0°, with the positive angle in the counterclockwise direction.

Figure 3 shows time waveforms for a single round burst from the Avenger. Figure 3(a) is from a microphone placed at 9.1 m (30 ft) from the gun muzzle at 30° from the firing direction. Figure 3(b) is from a microphone at the same distance at 90° from the firing direction. In Fig. 3(a), the initial pulse (0.008 s) in the waveform is the sonic boom from the projectile passing the microphone. This arrives before the muzzle blast at the microphone because of the supersonic velocity of the projectile. The largest peak (0.011 s) is the muzzle blast, which exceeds 3 kPa (0.44 psi), and is followed by the reflection of the sonic boom off of the gravel surface (0.012 s)

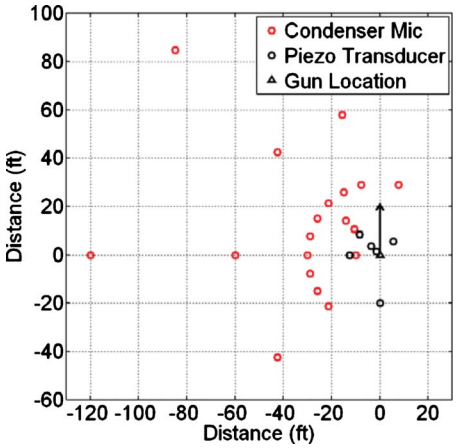

Fig. 2—Composite microphone setup for outdoor measurements. The muzzle is at the origin, and the black arrow denotes the firing direction.

and the ground-reflected muzzle blast (0.014 s). The ground-reflected sonic boom is louder than the direct sonic boom because of constructive interference with the blast wave. The effect of placing the microphones at 4.1 m (14 ft) above the ground can be observed in the time separation of the ground reflections from the direct field. Note that the 90° data do not contain a sonic boom because of the microphone position relative to the path of the projectile.

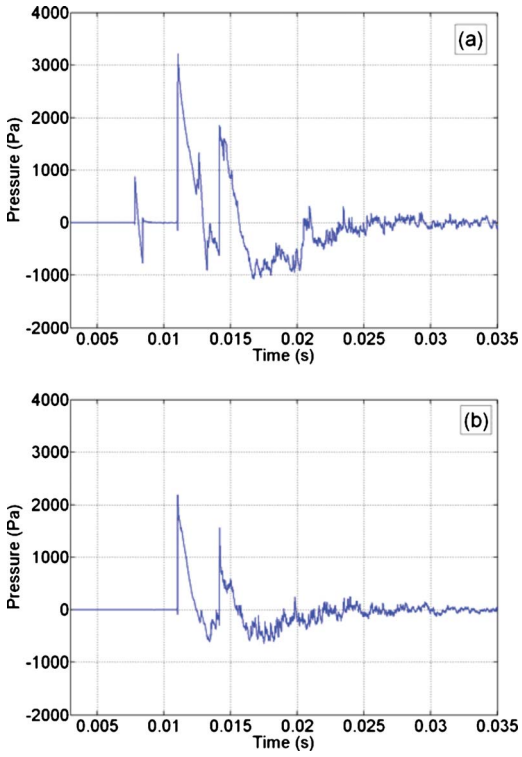

Fig. 3—Time waveform for a single shot, 30 ft away from the muzzle; (a) 30° from the firing direction; (b) 90° from the firing direction.

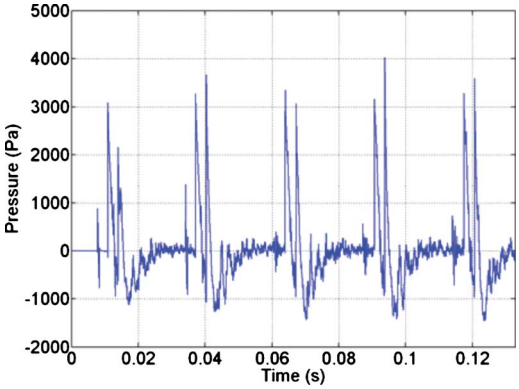

Fig. 4—Time waveform for a multi-round burst at half rate, 30 ft away from the muzzle, and 30° off of the firing direction.

A graph of the pressure for the first five rounds of a multi-round burst at half rate (35 rounds per second) is shown in Fig. 4. Note the sonic boom that arrives at the microphone before each muzzle blast. The changes in peak pressure between rounds and relative amplitudes of direct versus ground-reflected impulses can be attributed to a combination of muzzle blast variation, superposition of multiple blasts, finite sampling, and microphone effects, including diffraction from the angle of incidence and grid cap. However, these variations were consistent to within 1.6 dB of the average. The sonic boom from the last three rounds are much smaller and less distinct than the first two because of the turbulence introduced by the expulsion of hot gases from the gun. The waveforms are qualitatively similar to those shown in Refs. 9 and 10.

The direct muzzle blast pressures measured at the microphone arc at 9.1 m (30 ft) from the gun muzzle are displayed in Fig. 5. The peak pressures are shown as a function of angle for a single round, a 5-round, and a 15-round burst. The mean value and spread between minimum and maximum for the 5 and 15 round bursts are shown. The average values for the 5-round burst were used as an estimate for the direct-field muzzle blast peak pressures in investigating possible acoustical challenges and treatments for the range.

Several microphones and transducers were placed along lines at 45° and 90° off of the firing direction in order to measure the geometrical spreading of the muzzle blast. Given the shock-like features of the high-intensity blasts, it was expected that the peak pressure decay would be nonlinear, and consequently, greater than the inverse of the distance ($1/r$). According to theory[11], the peak amplitude for spherically spreading weak shocks as a function of distance is given by

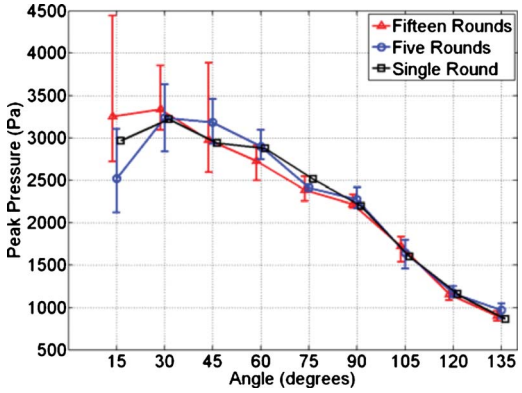

Fig. 5—Pressure vs. angle at 30 ft for a single round, a 5-round burst, and a 15-round burst. The markers represent the average (over all rounds) of the peak pressures of the direct sound at each angle. The error bars mark the maxima and minima of the peak pressures at each angle.

$$p_{sh}(r) = \frac{r_0 p_0}{r} \frac{\sqrt{1 + 2\eta \ln(r/r_0)} - 1}{\eta \ln(r/r_0)}, \qquad (1)$$

where $\eta = p_0 r_0 \beta / t_0 \rho_0 c_0^3$.

In Eqn. (1), r_0 and p_0 are the distance and pressure, respectively, at some initial point, r is the distance from the blast origin, β is the parameter of nonlinearity, t_0 is the initial e^{-1} decay time of the tail, ρ_0 is the ambient density, and c_0 is the speed of sound in air. Figure 6 shows a graph of the measured peak pressures versus distance for these two directions, along with curves showing $1/r$ and Eqn. (1). For Eqn. (1) in the graph, r_0 is 0.61 m (2 ft), p_0 is 120 kPa (17.4 psi, 195 dB), β is 1.2 (for air), t_0 is 0.4 ms, ρ_0 is 1.21 kg/m^3, and c_0 is 343 m/s. These data show the nonlinear decay, as expected.

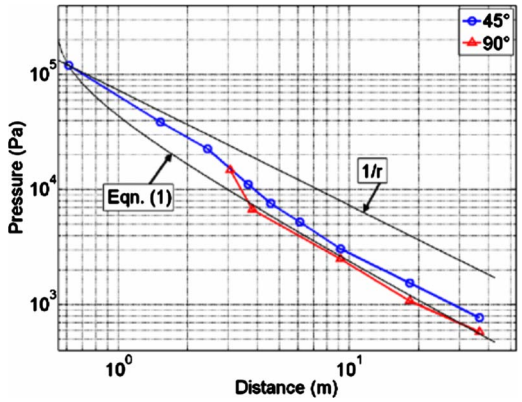

Fig. 6—Peak pressure vs. distance along lines 45° and 90° from the firing direction.

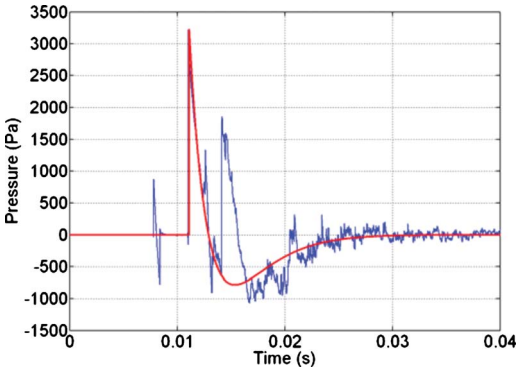

Fig. 7—Mathematical model of a single round from the gun plotted against an actual time waveform.

2.2 Mathematical Blast Wave

In order to further characterize the sound from the gun, a simulated 30-mm gun blast was developed. A typical blast waveform can be separated into two main parts: the rise and a damped exponential decay. The rise portion of a weak shock[11] can be modeled as

$$p(t) = \frac{1}{2} P^+ \{1 + \tanh[(2/t_{rise})t]\}, \qquad (2)$$

for $t=0$ occurring when the pressure is at half of its peak pressure, P^+. The rise time, t_{rise}, describes the change in time of a line that extends from zero pressure to the peak with the same slope as the waveform at $t=0$. The damped exponential decay portion of blast waveforms is commonly (and empirically) estimated using the modified Friedlander wave equation[12], given by

$$p(t) = P^+(1 - t/T^+)e^{-bt/T^+}. \qquad (3)$$

In Eqn. (3), which models the relaxation of the air after an explosion, T^+ is the amount of the time the waveform is positive, while the adjustable parameter b changes the duration of the negative portion of the waveform. Using these two equations, an ideal blast wave was created in MATLAB that modeled the waveform in Fig. 3. A graph of this theoretical wave is shown in Fig. 7 overlain on an actual time waveform measured from the gun. For the graph, t_{rise} is 8 μs, P^+ is 3221 Pa, T^+ is 1.8 ms, and b is 0.7. The rise time used is likely dominated by the response of the 6.35-mm microphone rather than actual absorptive processes. This MATLAB model was later used to simulate a multi-round burst pulse train and was convolved with impulse responses created from a computer model of the range (discussed below) in order to better study problem areas and the effectiveness of absorptive treatments in the range.

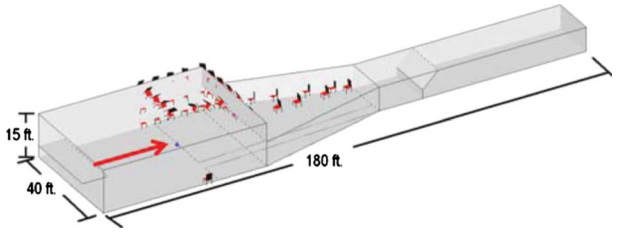

Fig. 8—Screenshot of the EASE model.

3 RANGE DESIGN

3.1 Dimensions

A computer model of the proposed firing range design was developed using EASE[13] and is displayed in Fig. 8. The large section of the room is 12.2 m (40 ft) wide, 4.7 m (15.3 ft) tall, and 18 m (59 ft) long. A door off the back platform leads to a hallway that connects the building entrance to the attached machine shop, and there are two pressure release vents (not included in the model) in the ceiling at each back corner. About 6.1 m (20 ft) in front of the gun muzzle, the ceiling drops to 2.6 m (8.5 ft) and the side walls begin to taper. The tunnel tapers from 12.2 m (40 ft) wide to 4.9 m (16 ft) over a section about 14.3 m (47 ft) long. At a distance of 4.6 m (15 ft) beyond the end of the tunnel, the bullets are captured by an 18.3-m (60-ft) depth gravel pit. At the end of the tunnel is a vent fan (not included in the model) that helps to circulate the air and expel dust and exhaust gases after firing. All of the walls, the ceiling, and the floor in the large section of the room are made of 30-cm (12-in) thick unfinished concrete, and most of the floor inside of the tunnel is 15 cm (6 in) of crushed rock gravel similar to the ground at the UTTR.

The 30-mm gun is situated in the middle of the large section of the range, approximately 1 m (3.5 ft) above the floor and 6.1 m (20 ft) behind where the ceiling drops and the tunnel begins. The gun muzzle is 6.1 m (20 ft) from either side wall. The 20-mm guns from both the F-16 and the AH-1 Cobra are tested from 3 m (10 ft) to the right of the 30-mm gun (10 ft from the wall). The planned F-22 20-mm gun mount will be 3 m (10 ft) to the left of the 30-mm gun.

3.2 Acoustical Considerations

An indoor Gatling gun range creates several potential acoustical challenges. Nearby faces and intersections, where pressure multiplies because of source imaging, are critical areas. Using peak pressures at 9.1 m (30 ft) from the outdoor experiments and Eqn. (1), estimates of the direct-field pressures at the walls and corners in the room can be obtained. Then, one must consider the pressure amplification that occurs at a boundary. For linear reflections at a perfectly hard surface, the pressure amplitude is double the free-field pressure at the surface. For nonlinear reflections, the amplification factor can exceed two[14]; however, only linear boundary interactions were considered in this study. At and near intersecting faces and interior corners, quadrupling and octupling of the free-field pressure can occur.

As an example, if we use 2.3 kPa (162 dB, 0.36 psi) as the peak pressure at 9.1 m (30 ft) at 90° from the firing axis (see Fig. 4), the expected free-field pressure at the side wall (6.1 m [20 ft]) will be 3.7 kPa (165 dB, 0.53 psi). Now, for this location, the ground reflection arrives about 1 ms after the initial blast, which is separated enough in time that it will not cause a significant increase in peak pressure. However, at the intersection of the side wall and the floor, the direct sound and the ground reflection will arrive simultaneously, causing pressure quadrupling. The expected peak pressure at this location would be about 15 kPa (177 dB, 2.1 psi).

Because of the muzzle blast's directionality, the face that drops from the ceiling is exposed to the maximum pressures created by the muzzle blast. Using the same method as above, the free-field pressure at the intersection of the ceiling and the front face is expected to exceed 4.3 kPa (166 dB, 0.62 psi). Pressure quadrupling suggests a pressure exceeding 17 kPa (178 dB, 2.5 psi) at that location, which is only slightly below the design threshold, without consideration of the ground or other reflections. Similarly, the pressures at the top interior corner (because of pressure octupling) would exceed 23 kPa (181 dB, 3.4 psi). Thus, even prior to considering multi-round bursts and room reverberation, there are some areas that would see pressures in excess of the 20-kPa (3-psi) design limit.

Other acoustical challenges include the converging tunnel and the room vents and exits. The tapered side walls create an acoustical focus on the ceiling between 9.1 and 12.2 m (30 and 40 ft) into the tunnel. At this location, the direct sound, the ground reflection, two reflections from the side wall, and the ground reflection off of the side walls all arrive at similar times. This effect was investigated using the EASE computer model. In addition, the room vents and exits will potentially transmit high noise levels outside the firing range, which could pose an auditory risk for personnel outside and in other areas of the building.

3.3 Computer Model

The EASE computer model of the test range was useful in guiding some of the acoustical recommendations. The model in Fig. 8 (with speaker representing the gun muzzle and the arrow showing the firing direction) was used to create impulse responses of the room at a number of listening positions (represented by the chairs). These impulse responses describe the behavior

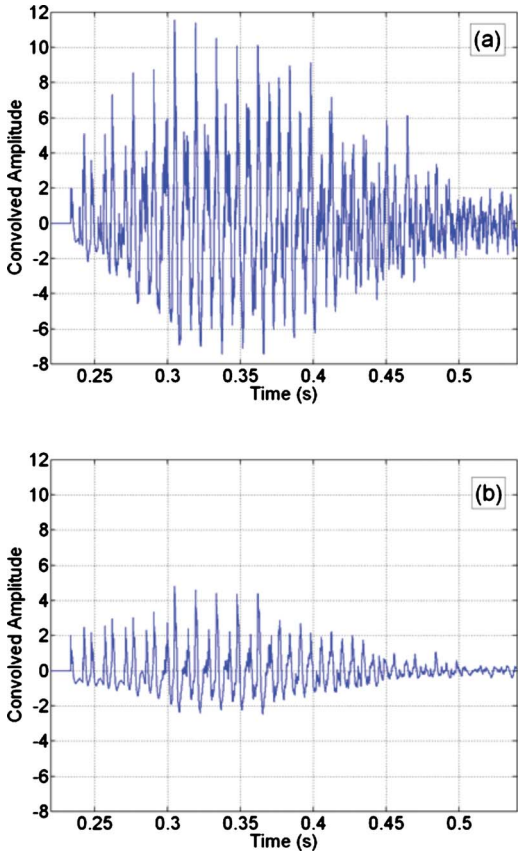

Fig. 9—Convolutions of the impulse response created in EASE at a position on the ceiling inside the converging tunnel with a 10-round pulse train; (a) Without absorption; (b) With absorption lining much of the walls and ceiling.

of sound within the range beginning from a source at the gun location. It must be noted that the results from the computer model are limited in some aspects. First, computations assume a linear regime, and the gun blast data clearly show nonlinearity. Second, EASE uses ray-tracing methods to create impulse responses and cannot account completely for reverberant energy. Third, the computational package does not predict the sound field that escapes out of the range through room vents and doors. Despite these limitations, the estimated impulse responses were useful in investigating some of the acoustical challenges described above and making recommendations rather than predicting exact pressures on a face.

Figure 9(a) is the convolution of the impulse response generated by EASE with a 10-round pulse train at full rate (70 rounds per second), created from the MATLAB model, for a location at the ceiling, 10.7 m (35 ft) into the converging tunnel. A multi-round burst was used to see the constructive interference of the direct and reverberant fields from successive rounds. The convolution shows an increase of a factor of more than ten relative to the free-field pressure, totaling pressures above 2 psi (177 dB, 14 kPa). Similar increases were observed at several of the locations described above, like the top interior corner and the dropped face in front of the gun.

In order to model the attenuation of the early reflections and reduce the reverberant energy in the room, a simulation was carried out which included the placement of 15 cm (6 in) of fiberglass insulation on the walls and ceiling from 1.5 m (5 ft) behind the firing line to 3 m (10 ft) inside the tunnel. Figure 9(b) shows the convolution for the same position after incorporating the fiberglass into the computer model. Note that the direct field amplitude remains unchanged, but many of the reflected peaks are significantly reduced in amplitude. Similar reductions were observed in the impulse responses and convolutions at other locations in the room. Simulations were also carried out to find the effectiveness of placing insulation farther down the tunnel, but it was determined that 3 m (10 ft) was sufficient to reduce the peak pressures below 3 psi on all surfaces. The results described above were used to guide the use of absorptive materials on the walls inside the range but indicated that a reduction of approximately 7 to 8 dB was theoretically possible.

3.4 Acoustical Treatments

Two possible treatments were explored to minimize incident pressures, reflections, and reverberant energy. As was tested in the computer model, wall and ceiling surfaces could be covered with a dense, absorptive material. While this will not be very effective for low-frequency noise, it will be effective in attenuating high frequencies, thereby reducing peak pressures of the gun blasts. Another possible treatment was an obstruction up close to the gun, some sort of muffler to attenuate the sound close to the source. A preliminary muffler design, which is not discussed in this paper, was tested during the outdoor measurements and showed an appreciable reduction in peak pressure.

For the wall treatments, HHI Corporation chose to use rock wool insulation. While rock wool and fiberglass have similar sound absorbing properties, rock wool is generally more fire-retardant and denser. Since rock wool is typically used to reduce reverberant energy rather than sound transmission, a simple insertion loss measurement was conducted in an anechoic chamber to find its transmission properties. The mathematical blast wave was played from a Mackie HR824 loudspeaker and recorded at a microphone about 30 cm (12 in) away. Then a 1.2-m by 1.8-m (4 ft by 6 ft) panel of rock wool insulation 15 cm (6 in) thick was placed between the speaker and the microphone so that the microphone was in the center of the panel. The

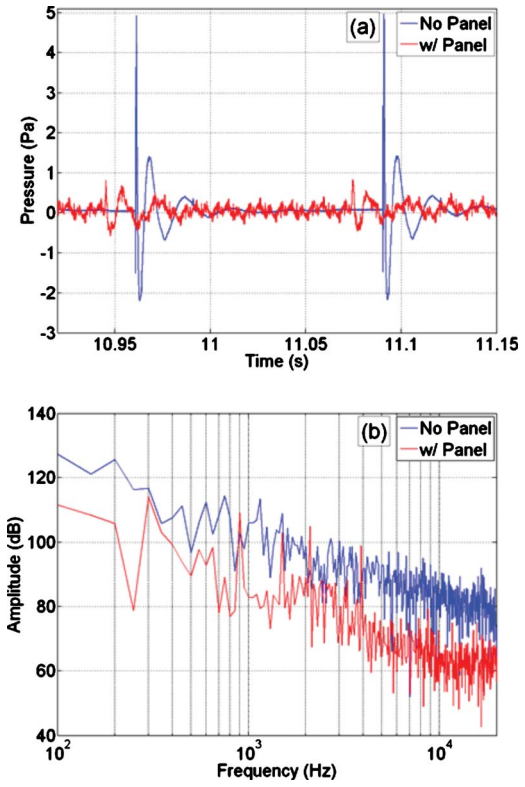

Fig. 10—Measured transmission of a blast wave through a panel of rock wool insulation; (a) Time waveforms; (b) Frequency spectra. The peaks are reduced by a factor of five (about 14 dB). Results above 20 kHz are not accurate because of the frequency response of the speaker.

panel was placed as close to the microphone as possible (about 5 cm, 2 in) in order to measure the transmitted blast with as little diffraction around the panel as possible. It must be noted that because the attenuation of intense sound waves through porous materials is amplitude-dependent[15], the results of this experiment could differ from those achieved inside the test range.

Figure 10 shows a comparison of the original wave to the transmitted wave and the frequency spectra of these waveforms. Note that the peaks were reduced by a factor of about five (about 14 dB), and the spectra show good absorption above 1 kHz, as expected. (Results above 20 kHz are not accurate because of the frequency response of the speaker.) The results of this experiment show that rock wool would be useful for reducing peak transmission to the concrete surface as well as early reflections and reverberant energy within the range. The walls and ceiling of the range were covered with 15 cm (6 in) of rock wool insulation from 1.5 m (5 ft) behind the firing line to 3 m (10 ft) into the tunnel.

In addition to the wall treatments, a steel-framed muffler constructed of 30-cm (12-in) deep rock wool

Fig. 11—Picture of the muffler built around the 30-mm gun, including microphones used for final measurements. The arrow is pointing at the microphone that recorded the data in Fig. 12.

insulation mounted on plywood and covered with steel mesh was built around and just forward of the 30-mm gun barrel (see Fig. 11). This further served to contain the muzzle blast.

4 FINAL MEASUREMENTS

Final measurements on the completed room were performed in April 2009. Two 20-mm guns and the 30-mm gun were fired, and the data were recorded using similar equipment as during the outdoor measurements. Microphones were placed at various locations inside and outside of the room. In order to check that peak pressures were below the 3-psi limit in critical areas, microphones were placed at the top interior corner, on the ceiling in the middle of the tunnel, and at the intersection of the wall and ceiling inside the tunnel. To measure the transmission loss from the rock wool insulation, microphones were placed in front of and behind the insulation on the side wall closest to the 20-mm gun. As with the outdoor gun characterization, piezoresistive transducers were placed up close to the guns to record peak levels. Microphones were also positioned on the roof near the pressure release vents, outside by the vent fan, in the hallway to the machine shop, and at the outside entrance to the building in order to compute exposure levels for personnel.

4.1 Inside the Range

Figure 12 shows a time waveform recorded 2.4 m (8 ft) from the muzzle of the 30-mm gun, behind the muffler. Note that the pressures are greatly reduced from the free-field pressures measured in the outdoor tests. This attenuation was also observed at other locations up close to the gun when the blasts transmitted through the muffler.

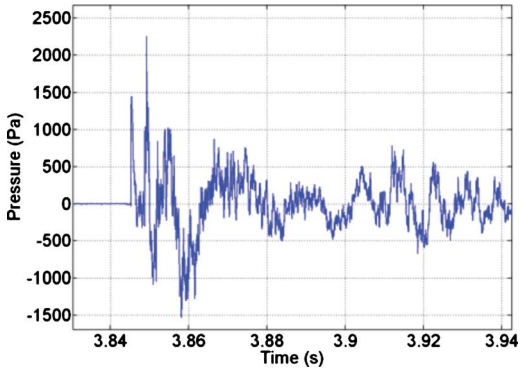

Fig. 12—Measured time waveform inside the range from a single round burst of the 30-mm gun from 2.4 m (8 ft) to the right of the muzzle (transmission through muffler). The arrow in Fig. 11 is pointing at this microphone.

Table 1 gives a list of peak pressures at various surfaces and intersections inside the room. The results show conclusively that peak pressures were well below the 3-psi design limit on all faces. The maximum pressure measured at the wall nearest to the 20-mm gun was 3100 Pa (164 dB, 0.45 psi). The peak pressures at the top interior corner and on the tunnel ceiling were clearly below the anticipated levels due to the acoustical treatments installed in the range. The highest pressures recorded in Table 1 were actually caused mainly by the sonic booms from the projectiles rather than the muzzle blasts. These larger pressures are results of amplification effects near a hard surface, an example of which can be seen in Fig. 13.

The reduction factor through the insulation was between three and four (about 10 to 12 dB) for all tests. A comparison of the recordings in front of and behind the insulation for a burst from the 20-mm gun is shown in Fig. 14, as well as the spectrum of each measurement. The spectra show absorption of more than 20 dB above

Table 1—Peak pressures inside of the room during multi-round bursts. All pressures are given in kPa (psi). The results indicate that all peak pressures were kept below the 3-psi *design limit.*

Location	20-mm Gun	30-mm Gun
Side wall, near 20-mm gun	3.10 (0.45)	1.64 (0.24)
Tunnel wall, near ceiling	12.4 (1.8)	5.98 (0.87)
Tunnel ceiling, center	6.49 (0.94)	10.2 (1.47)
Front face, ceiling corner	3.61 (0.52)	2.75 (0.40)
Back platform	1.91 (0.28)	2.31 (0.36)

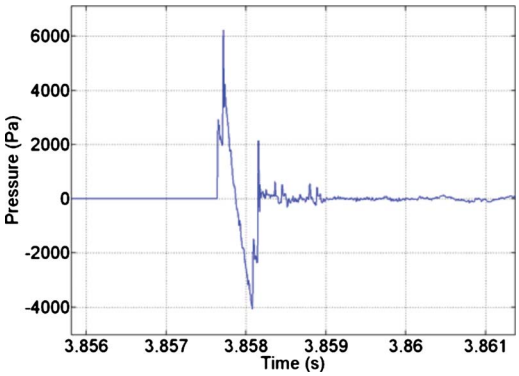

Fig. 13—Pressure doubling of the sonic boom from a 30-mm round on the ceiling inside the converging tunnel.

1 kHz. The rock wool sufficiently reduced the peak pressures on any surface to well below the 3-psi design limit.

4.2 Outside the Range

It was also necessary to ensure the adjacent machine shop could continue normal operation during firing.

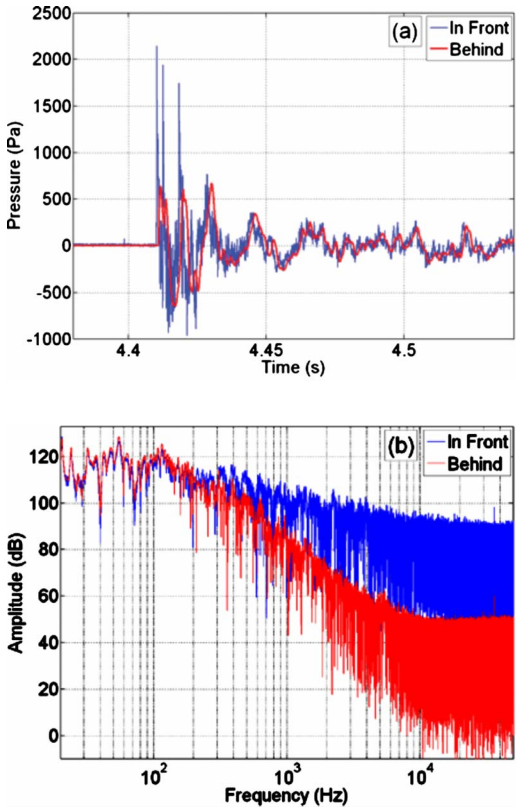

Fig. 14—Comparison of data in front of and behind rock wool insulation for a single round from the 20-mm gun inside the range; (a) Time waveforms; (b) Frequency spectra. The peaks were reduced by a factor of three (about 10 dB).

Table 2—Peak pressure levels (dB re 20 μPa*) and sound exposure levels (dBA and dBC) for a 50-round burst from the* 30-mm *gun.* 8-hour *equivalent noise levels* (Leq_A) *for a 50-round burst and a jet flyover are given for comparison. The peak pressures are well under the* 140 dB *peak limit set by OSHA.*

	Outside, entrance	Inside, hallway
Peak pressure level (dB)	121.8	112.4
A-weighted SEL (dBA)	94.9	85.9
C-weighted SEL (dBC)	110.5	99.8
8-hr. Leq_A (dBA)	50.3	41.3
8-hr. Leq_A for jet flyover (dBA)	57.4	40.2

Microphones were placed at the outside entrance of the building and in the hallway to the machine shop, as those locations are where workers would be most exposed to noise. Exposure levels were calculated to determine the possible auditory risks. Peak pressure levels (dB re 20 μPa) and A-weighted and C-weighted[16] sound exposure levels for a 50-round burst from the 30-mm gun are given for the two locations described above in Table 2. Eight-hour equivalent sound exposure levels (Leq_A) from the 50-round burst and from F-16 jet aircraft taking off nearby and flying overhead are also given for comparison. (For the data in Table 2, the hallway door leading to the outside was partially open.)

Note that the peak pressures both in the hallway and outside the main door are well under the 140 dB limit for impulsive noise given by the Occupational Safety and Health Administration (OSHA)[17]. The 8-hour equivalent shows that the overall exposure from one 50-round burst is relatively minimal. While one 50-round burst is much less than the daily expected testing in the range, several bursts of varying lengths would not increase exposure to levels near the 8-hour OSHA limit of 85 dBA[17]. From comparing equivalent exposure levels, noise from the gun was considered no more obtrusive than the noise produced by low-altitude jet aircraft.

5 CONCLUSIONS

The goals of this study were to characterize the sound from the 30-mm GAU-8 Avenger, reduce the incident pressure on any surface inside the test range to less than 3 psi, and verify that exposure levels were safe for workers. From measurements taken at the UTTR 30-mm gun test site, the muzzle blast was recorded, analyzed, and modeled using a rise time equation for weak shocks and the modified Friedlander wave equation. Measurements performed in the completed range verify that the installed acoustical treatments reduce incident pressures on all surfaces to below 3 psi. High-frequency absorption provided by rock wool insulation was found to be useful in reducing intense blast wave peak pressures, thereby limiting exposure of treated areas. Sound exposure levels for a 50-round burst were calculated for various locations outside of the test range and are safe for workers in the machine shop and around the test facility.

6 ACKNOWLEDGMENTS

Don Hokanson, Robert Smith, and Greg Crosby from HHI Corporation provided funding for and expertise during the project. Philip Roberts provided useful information regarding the structural aspects of the project. Several of the members of the BYU Acoustics Research Group were very helpful in performing both the preliminary and final measurements.

7 REFERENCES

1. E. M. Schmidt and D. D. Shear, “Optical measurements of muzzle blast”, *AIAA J.*, **13**(8), 1086–1091, (1975).
2. J. I. Erdos and P. D. Del Guidice, “Calculation of muzzle blast flowfields”, *AIAA J.*, **13**(8), 1048–1055, (1975).
3. K. S. Fansler, W. P. Thompson, J. S. Carnahan and B. J. Patton, “A parametric investigation of muzzle blast”, *Army Research Laboratory*, ARL-TR-227, (1993).
4. K. J. Kang, S. H. Ko and D. S. Lee, “A study on impulsive sound attenuation for a high-pressure blast flowfield”, *J. Mech. Sci. Technol.*, **22**(1), 190–200, (2008).
5. L. L. Pater and J. W. Shea, “Techniques for reducing gun blast noise levels: An experimental study”, *Naval Service Weapons Center*, NWSC-TR-81-120, (1981).
6. D. K. Kim and J. H. Han, “Establishment of gun blast wave model and structural analysis for blast load”, *J. Aircr.*, **43**(4), 1159–1168, (2006).
7. Mesa Corporation, *Final Report on* 30 mm *Gun Functional Range Relocation to Hill Air Force Base*, (1985).
8. Picture in public domain: http://en.wikipedia.org/wiki/File:GAU-8_meets_VW_Type_1.jpg.
9. B. Lipkens and D. T. Blackstock, “Model experiment to study sonic boom propagation through turbulence. Part I: General results”, *J. Acoust. Soc. Am.*, **103**(1), 148–158, (1998).
10. R. A. Lee and J. M. Downing, “Sonic boom produced by United States Air Force and United States Navy aircraft: measured data”, AL-TR-1991-0099, Wright-Patterson Air Force Base, (1991).
11. David T. Blackstock, Mark F. Hamilton and Allan D. Pierce, “Progressive waves in lossless and lossy fluids”, Ch. 4 in *Nonlinear Acoustics*, edited by Mark F. Hamilton and David T. Blackstock, Acoustical Society of America, Melville, New York, (2008).
12. Wilfred E. Baker, *Explosions in Air*, University of Texas Press, Austin, Texas, (1973).
13. Product of Renkus-Heinz, Inc. http://www.renkus-heinz.com/ease/index.html, accessed Aug 2010.
14. V. W. Sparrow and R. Raspet, “A numerical method for general

finite amplitude wave propagation in two dimensions and its application to spark pulses", *J. Acoust. Soc. Am.*, **90**(5), 2683–2691, (1991).
15. H. L. Kuntz and D. T. Blackstock, "Attenuation of intense sinusoidal waves in air-saturated, bulk porous materials", *J. Acoust. Soc. Am.*, **81**(6), 1723–1731, (1987).
16. P. D. Schomer, "High-energy impulsive noise assessment", *J. Acoust. Soc. Am.*, **79**(1), 182–186, (1986).
17. Occupational Safety and Health Standards Part 1910.95, Occupational Noise Exposure, Jun 1974; last amended Dec 08; http://www.osha.gov/pls/oshaweb/owadisp.show_document?p_table=standards&p_id=9735, accessed Aug 2010.